

# Epoxy resin modified with a thermoplastic

## Influence of modifier and reaction temperature on the phase separation

Joaquín López · Maite Rico · Carmen Ramírez ·  
Belén Montero

Japan Symposium 2008  
© Akadémiai Kiadó, Budapest, Hungary 2009

**Abstract** The effect of cure temperature and modifier proportion on the miscibility of an epoxy–amine system with a thermoplastic modifier was studied by analysis of phase diagrams, morphologies, and glass transitions. Phase diagrams for the system before and during reaction were obtained from a thermodynamic analysis of phase separation using a model based on Flory–Huggins theory. Different types of morphologies were observed and analyzed in function of cure temperature and modifier proportion. The validity of the thermodynamic model was checked by comparing with observed morphologies. Two glass transitions were observed for most of the modified systems indicating that a phase separation was occurred.

**Keywords** Thermoplastic/thermoset blends · Phase separation · Glass transition temperature · Morphology

### Introduction

The toughness of epoxy resins may be improved by the incorporation of thermoplastic components that are dispersed in the epoxy matrix. Such blends are usually prepared by the process known as Polymerization Induced Phase Separation (PIPS) [1, 2], in which the thermoplastic components are initially miscible with the monomers but are segregated during the curing of the epoxy resin.

Different types of morphologies can be generated by the PIPS process [3]: sea-island, nodular, bicontinuous, dual

phase, ribbonlike... The type of structure developed and their morphological characteristics (i.e., average size, distribution, and concentration of dispersed particles) will be determined by the proportion of modifier in the blend and the cure conditions used [4–6] (especially reaction temperature) which also will determine the conversion of phase separation. The final properties of modified resins depend largely on the developed morphology by materials and the nature of the separated phases [7–10], which may not be pure containing amounts of other component [11]. Therefore, the knowledge of the effects of polymerization temperature and modifier on the phase separation of system is essential to control the final properties of the modified materials.

The aim of the present work is to analyze the effect of polymerization temperature and modifier proportion on miscibility of a thermoplastic modifier/epoxy resin blend. The study of miscibility will be conducted by means of measures of cloud points with the construction of the corresponding phase diagrams, observation, and analysis of the morphologies developed and measures of glass transition temperatures.

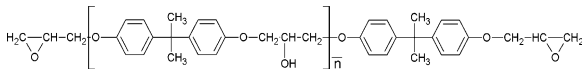
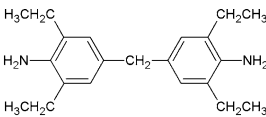
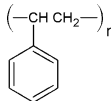
To obtain the phase diagrams, a thermodynamic analysis of phase separation for the system before and during the reaction at three cure temperatures was carried out, by means of a model based on the Flory–Huggins theory and the Koningsveld approach [12].

### Experimental

The epoxy–amine thermoset studied was constituted by stoichiometric amounts of a diglycidylether of bisphenol A (DGEBA) and an aromatic diamine, the 4,4′-methylenebis(2,6-diethylaniline) (MDEA). The thermoplastic modifier was a polystyrene (PS) with a polydispersity index of

J. López (✉) · M. Rico · C. Ramírez · B. Montero  
Departamento de Física, E.U.P. Ferrol, Universidad de A  
Coruña, Avda. 19 de Febrero s/n, 15405 Ferrol, Spain  
e-mail: labpolim@udc.es

**Table 1** Characteristics of the materials

Material	Supplier	Structure	Molar mass/g mol <sup>-1</sup>	Density/g cm <sup>-3</sup>
DGEBA	Ciba-Geigy Araldite GY260		376 $n = 0.13$	1.20
MDEA	Aldrich		310.5	1.35 <sup>a</sup>
PS	Aldrich		Mn = 140000 Mw = 230000	1.04

<sup>a</sup> From [17]

1.64. The chemical structures and characteristics of materials are shown in Table 1.

Temperatures of cloud point for the unreacted system,  $T_{cp}$ , and times of cloud point,  $t_{cp}$ , for the mixtures during the polymerization at three different temperatures (100, 120, and 140 °C) were determined using a light transmission device (He-Ne laser beam). Conversions of cloud point,  $pcp$ , of the mixtures reacting were calculated from measures of residual heats after  $t_{cp}$  and total heats by,

$$pcp = 1 - \frac{\Delta H_{RESIDUAL}}{\Delta H_{TOTAL}}$$

A differential scanning calorimeter (DSC-7, Perkin Elmer) was used to measure the glass transition temperatures and the heats of reaction [13]. Unreacted samples of about 5 mg were subjected to two successive scans in the DSC to a heating rate of 10 °C/min. The reaction enthalpies were calculated by integrating the exothermic peak obtained in the first scan and the glass transitions of cured materials were measured in the second scan. The morphologies were observed in a scanning electron microscope (SEM, JEOL JSM 6400).

The blends were prepared as follows: first, the PS was dissolved in the DGEBA using methylene chloride as a solvent which was later evaporated. In a second step, the PS/DGEBA blend was taken out of the oven and the corresponding amount of MDEA was added at room temperature, then stirring for 2 min.

Samples prepared in this way were tested to determine the cloud points, the reaction heats and the glass transition temperatures. To observe the morphologies, the samples were previously cured in an oven at studied temperatures, 100, 120, and 140 °C.

## Results and discussion

### Phase diagrams

To obtain the phase diagrams of our system of study, a thermodynamic analysis of phase separation was performed to the system before and during the polymerization by applying a model to the cloud-point curves obtained experimentally [14–16].

The model used is based on the Flory–Huggins Theory extended by the Koningsveld approach in which the components were taken as monodisperse species and the interaction parameter,  $\chi$ , was depending on temperature, composition, and conversion,  $\chi(T, \phi, p)$  [17, 18]. In this model, the Gibbs free energy of mixing per mol of unit cell ( $\overline{\Delta G}$ ) for a binary system is given by the following equation,

$$\overline{\Delta G} = RT \left[ \frac{\phi_1}{r_1} \ln \phi_1 + \frac{\phi_2}{r_2} \ln \phi_2 + g \phi_1 \phi_2 \right] \quad (1)$$

where, the subscripts 1 and 2, in our case, stand for the epoxy/amine pseudocomponent (stoichiometric DGEBA/MDEA system) and the thermoplastic modifier (PS) respectively;  $R$  is the gas constant;  $T$  is the absolute temperature;  $\phi_i$  is the volume fraction of  $i$  component;  $r_i$  is the relative size defined as the ratio of the molar volume of the  $i$  component with respect to a reference volume ( $V_{ref}$ ), as reference volume was taken the molar volume of the monomer of PS ( $V_{ref} = 100 \text{ cm}^3 \text{ mol}^{-1}$ ).  $g$  is a function depending on the temperature and composition for an unreacted mixture, which is related to the interaction parameter  $\chi(T, \phi_2)$  through the following expression,

$$\chi(T, \phi_2) = g(T, \phi_2) - \frac{\partial g(T, \phi_2)}{\partial \phi_2} \phi_1 \quad (2)$$

In this work, as usual [19–21],  $\chi(T, \phi_2)$  was defined as the product of a temperature dependent term,  $D(T)$ , and a concentration dependent term,  $B(\phi_2)$ , given by,

$$\chi(T, \phi_2) = D(T) \times B(\phi_2) = \left( A + \frac{B}{T} \right) \times \frac{1}{1 - c\phi_2} \quad (3)$$

where  $A$ ,  $B$ , and  $c$  are adjustable model parameters.

For a system reacting,  $\chi$  can also be a function of conversion,  $\chi(T, \phi_2, p)$ . The effect of conversion on interaction parameter can be considered by making the adjustable model parameters ( $A$ ,  $B$ ,  $c$ ) not constant and varying with conversion [22, 23].

During reaction, the relative average size of the epoxy/amine component ( $r_1$ ) does not remain constant but increases with conversion as follows [24],

$$r_1(p) = \left( 1 - \frac{4p}{3} \right)^{-1} \times \frac{V_1}{V_{\text{ref}}} \quad (4)$$

where  $V_1$  is the molar volume of the epoxy/amine pseudocomponent at zero conversion.

The binodal curves, spinodal curves, and critical points were calculated using the standard procedures [25], which involve determining the interaction parameters by applying the model to the experimental cloud-point curves (CPC) of the system without reaction and during the reaction. For that, first the dependence of  $\chi$  with temperature and composition was determined from analysis of unreacted system and then it was used for the analysis of system reacting, calculating the dependence of  $\chi$  with conversion. Once the total dependence of  $\chi$ ,  $\chi(T, \phi_2, p)$ , was known, the phase diagrams were plotted. The numerical solution was obtaining using the Mathcad 11 program.

The experimental cloud-point curve for the PS + epoxy/amine system before reaction is shown in Fig. 1, indicating an upper critical solution temperature (UCST) behavior.

The fitting of the CPC by the thermodynamic model led to an interaction parameter for the unreacted system given by,

$$\chi(T, \phi_2) = \left( 0.0805 + \frac{33.680}{T} \right) \times \frac{1}{1 - 0.651 \times \phi_2} \quad (5)$$

From this dependence of  $\chi$  with temperature and composition, the binodal curve, the spinodal curve, and the critical point for the system without reaction were obtained and are also shown in Fig. 1. The calculated critical composition is close to 16.1% in volume of PS.

The experimental cloud-point curves obtained for the system during reaction at 100, 120, and 140 °C are shown in Fig. 2. The increase of the reaction temperature shifted

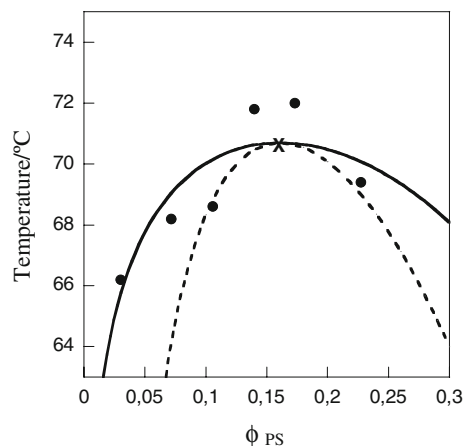


**Fig. 1** Phase diagram for the PS + DGEBA/MDEA (1:1) system without reaction: experimental cloud-point data (circle), calculated binodal curve (solid line), spinodal curve (dotted line), and location of critical point (times)

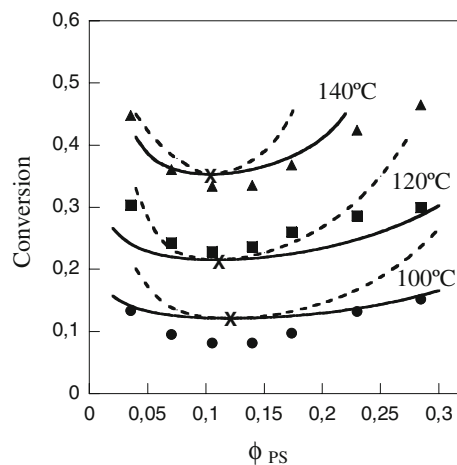


**Fig. 2** Phase diagrams for the PS + DGEBA/MDEA (1:1) system during reaction at three different temperatures: experimental cloud-point conversion at 100 °C (circle), 120 °C (square), and 140 °C (triangle), with the corresponding calculated binodal curves (solid line), spinodal curves (dotted line), and location of critical points (times)

the cloud-point conversion (pcp) upwards, increasing the miscibility of system. This is typical of UCST behavior. The fitting of the CPCs by the thermodynamic model and the use of the dependence  $\chi(T, \phi_2)$  determined for the unreacted system led to the following interaction parameter for the system reacting,

$$\chi(T, \phi_2, p) = \left( 0.0805 - 0.142p - 0.103p^2 + \frac{33.680}{T} \right) \times \frac{1}{1 - (0.651 - 0.498p) \times \phi_2} \quad (6)$$

Introducing  $\chi(T, \phi_2, p)$  (Eq. 6) in the equations for calculating the phase equilibria, spinodal curve, and critical

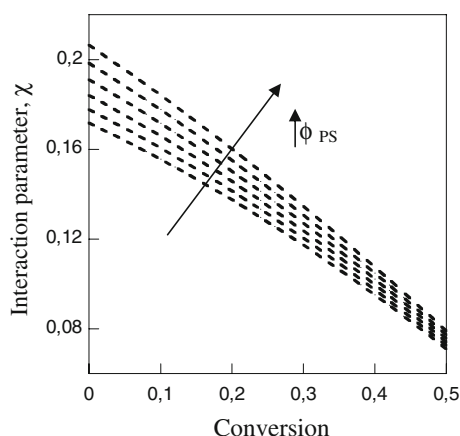


**Fig. 3** Variation of the interaction parameter,  $\chi$ , with conversion at 100 °C for different compositions of PS (0–30 vol% PS) increasing in the direction of the arrow

point and solving, the phase diagram during the reaction was traced by following the usual procedure.

Figure 2 also shows the phase diagrams obtained for the system reacting at the three studied temperatures, with the binodal and spinodal curves and the critical points resulting from applying the thermodynamic model. A good agreement for the cloud-point curves calculated theoretically (binodal curves) and the ones determined experimentally was obtained. The resulting critical compositions expressed in volume fraction of PS were 0.120, 0.109, and 0.104 (8.9, 9.3, and 10.3% in mass of PS) for the system curing at 100, 120, and 140 °C, respectively.

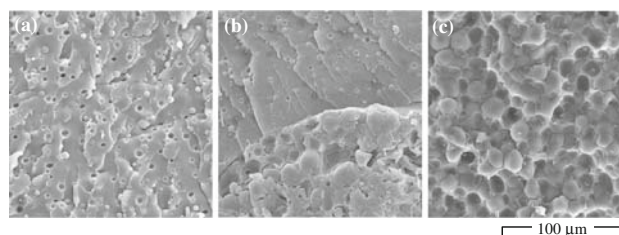
An analysis of the variation in the interaction parameter with conversion was carried out to find out the role of  $\chi$  in the phase separation. It is shown in Fig. 3.

Figure 3 shows that the interaction parameter decreases when the reaction advances for any composition. This effect is more drastic for higher PS proportions. This means that PS was more compatible with reactive oligomeric species than with the mixture of starting monomers, favoring miscibility. However the phase separation was produced due to that the main driving force of the demixing process is the increase in the size of the thermosetting oligomer, which decrease the entropic contribution to the free energy of mixing [26].

### Morphologies

Three different types of morphologies were observed depending mainly on the initial PS proportion. They are shown in Fig. 4.

Thus, the blends with 3 and 6% in mass of PS showed a sea-island morphology (Fig. 4a) consisting in spherical thermoplastic domains dispersed in an epoxy-rich matrix. The blends with 15, 20, and 25% in mass of PS showed an



**Fig. 4** SEM micrographics of PS + DGEBA/MDEA (1:1) system cured at 100 °C with different proportions of PS: **a** 6, **b** 12, and **c** 20 wt% PS

inverted morphology (nodular morphology, Fig. 4c) where nodular epoxy particles are dispersed in a thermoplastic matrix. And blends with 9 and 12% in mass of PS showed a complex morphology, known as dual-phase morphology (Fig. 4b) consisting of macroscopic domains of both, sea-island and nodular structures. This dual morphology is typical of compositions near the critical point [27–30], where a reversal in the nature of the separated phases is produced.

The possible range for the critical composition shown by the morphologies was between the compositions where sea-island and nodular morphologies were observed (between 6 and 15% in mass of PS) regardless of cure temperature in the range of temperatures studied.

The results of thermodynamic analysis of phase separation were correlated with the observed morphologies, resulting that the critical compositions obtained thermodynamically resulted were within the range possible shown by the morphologies and very close to the compositions that showed dual-phase morphology. Therefore, a good accordance was obtained between both thermodynamics and morphological results, which indicates the validity of model and approaches used.

Moreover, the effects of cure temperature and initial modifier proportion on morphologies were analyzed and discussed [31]. Figure 5 shows the influence of both, cure temperature and PS proportion on the sea-island and nodular morphologies.

Two morphological parameters were determined for each morphology with the aid of an image analyzer program (UTHCSA Image Tool 3.00): average diameter of dispersed particle,  $\bar{D}$  ( $\mu\text{m}$ ) and number of dispersed particles for unit area,  $\bar{N}$  ( $\text{part } \mu\text{m}^{-2}$ ). The results are shown in Table 2 for the size of particle ( $\bar{D}$ ) and in Fig. 6 for the concentration of particles ( $\bar{N}$ ).

For the blends showing sea-island morphology, both the size and the concentration of dispersed particles increased with the initial PS proportion. This is due to the increasing onset conversion that leads to a greater volume of dispersed phase. For this morphology, an increase in cure temperature caused a major number of dispersed particles but the size of particle decreased. This trend can be explained

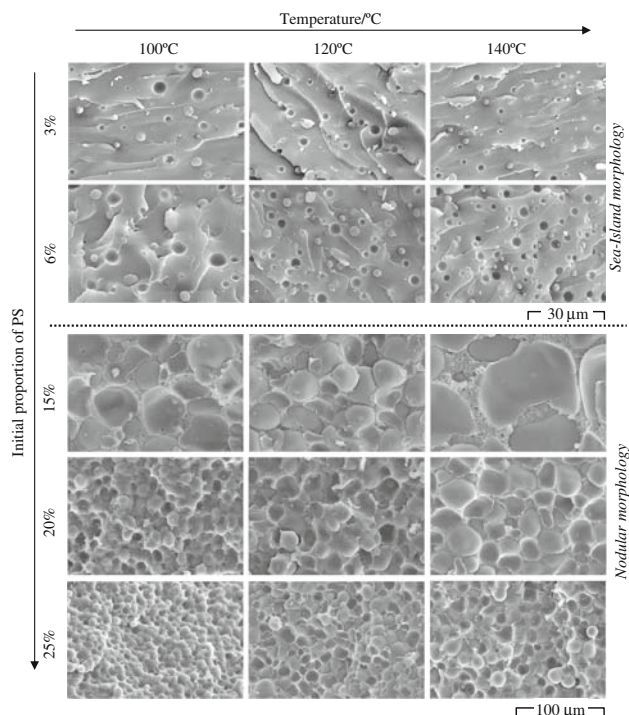


**Fig. 5** Morphologies obtained for the PS + DGEBA/MDEA (1:1) system cured at different temperatures and with various proportions of modifier

because increasing the cure temperature the cloud-point conversion increases, as shown in the phase diagram (Fig. 2), leading to an increase in the viscosity of the epoxy matrix which hinders mass transfer favoring the formation of more but smaller particles.

For the blends with nodular morphology, an increase in the PS proportion or a decrease in temperature led to a decrease in the average size and an increase in the number of dispersed particles.

For the blends showing dual-phase morphology the increase of PS caused that the proportion of nodular structure increased and the one of sea-island decreased while the

**Table 2** Average diameter of dispersed particles,  $\bar{D}$ , for the morphologies of the DGEBA/MDEA (1:1) modified with different proportions of PS and at various temperatures

%PS	$\bar{D}/\mu\text{m}$		
	100 °C	120 °C	140 °C
Sea-island morphology			
3	2.9 ± 1.4	2.6 ± 0.9	2.0 ± 0.7
6	3.5 ± 1.5	3.0 ± 1.0	2.6 ± 0.8
Nodular epoxy morphology			
15	30 ± 9	46 ± 12	90 ± 30
20	15 ± 4	23 ± 5	29 ± 8
25	7 ± 2	12 ± 4	15 ± 4

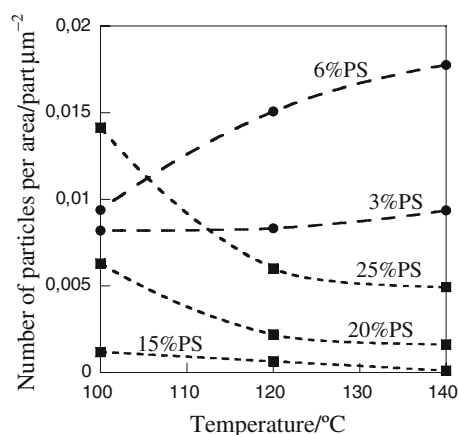


**Fig. 6** Concentration of dispersed particles for the PS + DGEBA/MDEA (1:1) system cured at different temperatures and with various proportions of PS: *circle* for compositions showing sea-island morphology and *square* for compositions showing nodular morphology

cure temperature does not seem to have much effect on the morphology in the studied range.

#### Glass transition temperatures

The miscibility of PS with the DGEBA/MDEA system was studied by means of measuring the glass transitions temperatures of the cured blends [32–34].

The values of glass transition temperature ( $T_g$ ) and change in specific heat at the glass transition ( $\Delta C_p$ ) obtained for the different modified systems are reflected in Table 3. The corresponding values for pure components, i.e. DGEBA/MDEA system and PS, are also listed.

Most of the modified system showed two glass transitions temperatures next to those of the pure components. This indicates that a phase separation has occurred leading to two separated phases, one rich in the thermoset and the other rich in the modifier.

**Table 3** Glass transition temperature ( $T_g$ ) with the corresponding change of specific heat ( $\Delta C_p$ ) for blends of DGEBA/MDEA and PS in different proportions

%PS	PS-rich phase		Epoxy-rich phase	
	$T_g/^\circ\text{C}$	$\Delta C_p/\text{J g}^{-1} \text{ }^\circ\text{C}^{-1}$	$T_g/^\circ\text{C}$	$\Delta C_p/\text{J g}^{-1} \text{ }^\circ\text{C}^{-1}$
0	–	–	146.18	0.317
3	–	–	146.08	0.310
6	–	–	145.87	0.304
9	–	–	145.74	0.287
12	105.96	0.075	144.72	0.274
15	105.89	0.101	144.39	0.257
20	105.49	0.124	143.84	0.246
25	104.55	0.139	142.41	0.229
100	100.11	0.288	–	–



For the blends with a lower percentage of 12 wt% PS, only the glass transition corresponding to thermoset-rich phase could be distinguished. This is because the amount of PS-rich phase is very small, making the signal corresponding to its glass transition is not detected by DSC.

Increasing the PS proportion in the system, the temperature and the change of specific heat at the glass transition for the thermoset-rich phase decreased while those for the PS-rich phase increased. The variation in  $T_g$  of each phase can be attributed to that phases are not pure but dissolve some of the other component. The variation in the change of specific heat is due to that the intensity of  $\Delta C_p$  in a phase depends on the mass fraction of that phase. Then, increasing the modifier content, the fraction of PS-rich phase increases and consequently its  $\Delta C_p$ , while the fraction of thermoset-rich phase decreases, making the  $\Delta C_p$  smaller.

Despite these variations, the glass transition temperatures of the modified system were very similar to those of the pure components. This means that a nearly complete phase separation has occurred and that only small amounts of other component remained dissolved in each phase at the end of the reaction.

## Conclusions

A study of the miscibility of a polystyrene with an epoxy-amine system in function of the initial PS proportion and the polymerization temperature was realized through analysis of the phase diagrams, morphologies, and glass transition temperatures.

The studies showed that a phase separation took place during polymerization (PIPS) in the modified systems leading to heterogeneous systems consisting of two separated phases. Cloud-point curves experimentally measured showed that the system is characterized by an upper critical solution temperature behavior, where the conversion of phase separation (i.e. miscibility) increased with the cure temperature.

The phase diagrams for the system before and during polymerization at three cure temperatures were obtained from a thermodynamic analysis of phase separation. This analysis was conducted using a model based on the Flory–Huggins theory where the components were considered as monodisperse and the interaction parameter was dependent on temperature, composition, and conversion. The interaction parameter decreased with the advance of conversion favoring the miscibility of system. However the phase separation is caused because the increase in the size of thermoset is the main force of the demixing process.

Three types of morphologies were observed depending on the initial proportion of PS: sea-island morphology for low PS proportion, nodular morphology for high PS

proportion ( $\geq 15$  wt% PS), and dual-phase morphology for blends of 9 and 12 wt% PS.

The critical points theoretically obtained for the system reacting were within the range possible shown by the morphologies (between 6 and 15% in mass of PS) indicating the validity of the model and approaches used.

The effect of cure temperature and PS composition on the size and concentration of dispersed particles was analyzed for each of the morphologies. An increase in temperature affected in the opposite way to the morphologies: thus, for the sea-island morphology, it increased the concentration of dispersed particles and decreased the particle size, while for nodular morphology, it decreased the concentration of particles but increased its size. Cure temperature had little effect on dual-phase morphology.

An increase in PS proportion for the nodular morphology led to a greater number of dispersed particles but they are smaller while for sea-island morphology, both the size and concentration of dispersed particles increased. For dual-phase morphology, an increase in the modifier content led to increase in the proportion of nodular structure and a decrease in sea-island structure.

Two glass transition temperatures were observed for most of the modified systems indicating the existence of two separated phases. These  $T_g$  were close to those of pure components, therefore, only small amounts of other component remained dissolved in each phase at the end of reaction.

**Acknowledgements** The financial support of the Ministerio de Educación y Ciencia (CICYT MAT2007-61677) is gratefully acknowledged.

## References

1. Williams RJJ, Rozenberg BA, Pascault JP. Reaction-induced phase separation in modified thermosetting polymers. In: Koenig JL, editor. *Advances in polymer science vol 128: polymer analysis, polymer physics*. Berlin: Springer; 1997. p. 95–156.
2. Pascault JP, Williams RJJ. Formulation and characterization of thermoset-thermoplastic blends. In: Paul DR, Bucknall CB, editors. *Polymer blends volume 1: formulation*, chap 13. New York: Wiley; 2000. p. 379–415.
3. Park JW, Kim SC. Phase separation during synthesis of polyetherimide/epoxy semi-IPNs, Chap 2. In: Kim SC, Sperling LH, editors. *IPNs around the world*. Chichester: Wiley; 1997. p. 27–48.
4. Verchere D, Pacault JP, Sautereau H, Moschiar SM, Riccardi CC, Williams RJJ. Rubber-modified epoxies II. Influence of the cure schedule and rubber concentration on the generated morphology. *J Appl Polym Sci*. 1991;42:701–16.
5. Remiro PM, Marieta C, Riccardi CC, Mondragon I. Influence of curing conditions on the morphologies of a PMMA-modified epoxy matrix. *Polymer*. 2001;42:9909–14.
6. Auad ML, Borrajo J, Aranguren MI. Morphology of rubber-modified vinyl ester resins cured at different temperatures. *J Appl Polym Sci*. 2003;89:274–83.

7. Auad ML, Frontini PM, Borrajo J, Aranguren MI. Liquid rubber modified vinyl ester resins: fracture and mechanical behavior. *Polymer*. 2001;42:3723–30.
8. Auad ML, Proia M, Borrajo J, Aranguren MI. Rubber modified vinyl ester resins of different molecular weights. *J Mater Sci*. 2002;37:4117–26.
9. Auad ML, Borrajo J, Aranguren MI. Relation between morphology and thermal, mechanical and fracture properties in rubber modified divinylester resins. In: Zaikov GE, Monakov YB, Jimenez A, editors. *Homolytic and heterolytic reactions: problems and solutions*, Chap 7. Hauppauge: Nova Science Publishers, Inc.; 2004. p. 175–95.
10. Zucchi IA, Galante MJ, Williams RJJ. Comparison of morphologies and mechanical properties of crosslinked epoxies modified by polystyrene and poly(methyl methacrylate) or by the corresponding block copolymer polystyrene-*b*-poly(methyl methacrylate). *Polymer*. 2005;46:2603–9.
11. Fang DP, Frontini PM, Riccardi CC, Williams RJJ. Rubber-modified thermosets cured in heated molds: experimental study of phase separation profiles. *Polym Eng Sci*. 1995;35(17):1359–68.
12. Koningsveld R, Kleintjens LA. Liquid–liquid phase separation in multicomponent polymer systems. X. Concentration dependence of the pair-interaction parameter in the system cyclohexane-polystyrene. *Macromolecules*. 1971;4:637–41.
13. López J, Rico M, Montero B, Díez J, Ramírez C. Polymer blends based on an epoxy-amine thermoset and a thermoplastic. *J Therm Anal Calorim*. 2009;95(2):369–76.
14. Rico M, Borrajo J, Abad MJ, Barral L, López J. Thermodynamic analysis of phase separation in an epoxy/polystyrene mixture. *Polymer*. 2005;46:6114–21.
15. Soulé ER, Jaffrennou B, Méchin F, Pascault JP, Borrajo J, Williams RJJ. Thermodynamic analysis of the reaction-induced phase separation of solutions of random copolymers of methyl methacrylate, *N,N*-dimethylacrylamide in the precursors of a polythiourethane network. *J Polym Sci B*. 2006;44:2821–7.
16. Maiez-Tribut S, Pascault JP, Soulé ER, Borrajo J, Williams RJJ. Nanostructured epoxies based on the self-assembly of block copolymers: a new miscible block that can be tailored to different epoxy formulations. *Macromolecules*. 2007;40:1268–73.
17. Riccardi CC, Borrajo J, Meynie L, Fenouillot F, Pascault JP. Thermodynamic analysis of the phase separation during the polymerization of a thermoset system into a thermoplastic matrix. Effect of composition on cloud-point curves. *J Polym Sci B*. 2004;42:1351–60.
18. Zucchi IA, Galante MJ, Borrajo J, Williams RJJ. A model system for the thermodynamic analysis of reaction-induced phase separation: solutions of polystyrene in bifunctional epoxy/amine monomers. *Macromol Chem Phys*. 2004;205:676–83.
19. Qian C, Mumby SJ, Eichinger BE. Phase diagrams of binary polymer solutions and blends. *Macromolecules*. 1991;24:1655–61.
20. Choi JJ, Bae YC. Liquid–liquid equilibria of polydisperse polymer systems: applicability of continuous thermodynamics. *Fluid Phase Equilib*. 1999;157:213–28.
21. Jaffrennou B, Soulé ER, Méchin F, Borrajo J, Pascault JP, Williams RJJ. Miscibility of blends of poly(methyl methacrylate) and oligodiols based on a bisphenol A nucleus and ethylene oxide or propylene oxide branches. *Polymer*. 2004;45:7185–92.
22. Borrajo J, Riccardi CC, Williams RJJ, Cao ZQ, Pascault JP. Rubber-modified cyanate esters: thermodynamic analysis of phase separation. *Polymer*. 1995;36(18):3541–7.
23. Soulé E, García de la Mata M, Borrajo J, Oyanguren PA, Galante MJ. Reaction-induced phase separation in an epoxy/low molecular weight solvent system. *J Mater Sci*. 2003;38:2809–14.
24. Ruseckaite RA, Williams RJJ. Castor-oil-modified epoxy resins as model systems of rubber-modified thermosets 1: thermodynamic analysis of the phase separation. *Polym Int*. 1993;30:11–6.
25. Kamide K, Matsuda S, Shirataki H. Comparison of two direct methods for estimating the cloud point curve of quasi-binary systems consisting of multicomponent polymers dissolved in a single solvent. *Eur Polym J*. 1990;26(4):379–91.
26. Riccardi CC, Borrajo J, Williams RJJ, Girard-Reydet E, Sauteureau H, Pascault JP. Thermodynamic analysis of the phase separation in polyetherimide-modified epoxies. *J Polym Sci B*. 1996;34:349–56.
27. Oyanguren PA, Galante MJ, Andromaque K, Frontini PM, Williams RJJ. Development of bicontinuous morphologies in polysulfone-epoxy blends. *Polymer*. 1999;40:5249–55.
28. Hoppe CE, Galante MJ, Oyanguren PA, Williams RJJ, Girard-Reydet E, Pascault JP. Transparent multiphase polystyrene/epoxy blends. *Polym Eng Sci*. 2002;42(12):2361–8.
29. Arribas C, Masegosa RM, Salom C, Arévalo E, Prolongo SG, Prolongo MG. Epoxy/poly(benzyl methacrylate) blends: miscibility, phase separation on curing and morphology. *J Therm Anal Calorim*. 2006;86(3):693–8.
30. Prolongo MG, Arribas C, Salom C, Masegosa RM. Mechanical properties and morphology of epoxy/poly(vinyl acetate)/poly(4-vinyl phenol) brominated system. *J Therm Anal Calorim*. 2007;87(1):33–9.
31. Prolongo SG, Buron M, Salazar A, Urena A, Rodriguez J. Morphology and dynamic mechanical properties of epoxy/poly(styrene-co-allyl alcohol) blends. *J Therm Anal Calorim*. 2007; 87(1):269–76.
32. MacKnight WJ, Karasz FE, Fried FR. Solid state transition behavior of blends, chap 5. In: Paul DR, Newman S, editors. *Polymer blends*. San Diego: Academic Press; 1978. p. 185–224.
33. Del Río C, Acosta JL. Determination of the interaction parameter of partially or totally compatible systems through glass transition temperature measurements. *Eur Polym J*. 1996;32(7):913–7.
34. Radhakrishnan CK, Sujith A, Unnikrishnan G. Thermal behaviour of styrene butadiene rubber/poly(ethylene-co-vinyl acetate) blends TG and DSC analysis. *J Therm Anal Calorim*. 2007;90(1): 191–9.